2013

# Mimicking the Binding and Unbinding of Fe3+ With Transferrin Using A Single Biomimetic Nanochannel

Chao Zhao
Xiaosi Li
Lingyan Li
Xiong Gong
Yung Chang, et al.

ChemComm

RSC Publishing

COMMUNICATION

# Mimicking the binding and unbinding of $Fe^{3+}$ with transferrin using a single biomimetic nanochannel†

Cite this: *Chem. Commun.*, 2013, **49**, 9317

Received 5th June 2013,
Accepted 8th August 2013

DOI: 10.1039/c3cc44249g

www.rsc.org/chemcomm

Chao Zhao,[a] Xiaosi Li,[a] Lingyan Li,[a] Xiong Gong,[b] Yung Chang[c] and Jie Zheng*[a]

**A new type of apo-Tf functionalized nanochannel is developed to achieve the specific and selective binding and unbinding of $Fe^{3+}$ in a multiple and reversible manner *via* a protein-conformation-gating mechanism. This ion-responsive biomimetic nanochannel provides a simple, robust, and promising model for studying other biological processes.**

Biological ion channels that regulate ion transport and ion selectivity through cell membranes are the basis of many physiological processes in a living organism.[1] Due to the complexity of cell membranes and the limited structural information of ion channels, it is a still very challenging task to study ion transport properties of ion channels *in vitro*. Recently, development of artificial biomimetic nanochannels as a substitution of ionic channels provides promising model systems to replicate, enhance, and better understand the functionality of these biological channels.[2] Unlike most fragile and complex biological ion channels, artificial biomimetic nanochannels offer several advantages for the fundamental study of different complex biological processes:[3] (1) the nanochannels are usually mechanically and chemically robust, with well-defined channel structures;[4] (2) the nanochannels can specifically mimic certain important functions of ionic channels in cell membranes by isolating other uncertain membrane components; and (3) most importantly, the nanochannels can be readily modified with functional molecules at the inner wall to produce stimuli-response nanochannels for biosensors,[5] molecular filtration,[6] and nanofluidic devices.[7] Thus, a comprehensive understanding of ion behaviors (*i.e.* ionic selectivity, rectification, and gating) in synthetic nanochannels increases our fundamental knowledge of physiological processes in biological ionic channels, but also facilitates the development of practical nanofluidic/nanosensor devices for various biomedical applications.

A number of fabrication methods (*i.e.* biological molecule self-assembly,[8] electrochemical etching,[9] the anodic oxidation method,[10] electron beam and laser,[11] and ion-track-etching[12]) have been developed to produce single or multiple biomimetic nanochannels of different sizes and shapes. These biomimetic nanochannels have achieved their functions to sense metal ions,[5,13,14] to sequence DNA,[3] to scrutinize proteins,[15] and to mimic some biological processes.[5] A single nanochannel presents a perfect model system for the fundamental study of nanochannel behaviors, while multiple nanochannels are more convenient for large-scale, real-world applications.

Here we developed a single biomimetic iron-responsive nanochannel to conveniently mimic a multiple and reversible binding and unbinding process between irons and the apo-transferrin conjugated nanochannel. Human transferrin (Tf), an iron-binding protein of 80 kDa consisting of two specific high-affinity $Fe^{3+}$ binding sites, functions in binding and delivery irons to supply the needs of iron-dependent cells bearing the specific transferrin receptor (TfR) *via* a receptor-mediated endocytosis process.[16] Tf has two states under physiological conditions: an iron-bound state of "holo-transferrin" (holo-Tf) and a free-iron-bound state of "apo-transferrin" (apo-Tf). Molecular details of Tf to bind and release irons have been well studied, including the solved atomic structures of Tf at the iron binding and release states. However, it still remains a mystery how Tf can repeat 100–200 cycles of reversible iron uptake and delivery during its lifetime of 16 days *in vivo*.[17] This multiple, reversible, iron-binding–unbinding process has never been realized *in vitro*. It is highly desirable but challenging to develop a nanochannel system that can switch reversibly between iron binding and releasing states to mimic this iron-transferrin binding–unbinding process. To our knowledge, as compared to other ion-responsive nanochannels using DNA, peptide, or polymer as responsive coatings, we are the first to report a protein-based nanochannel capable of switching repeatedly between iron-binding and iron-release states to achieve multiple iron binding and releasing events in a controlled manner (Fig. 1).

Here, a single conical nanochannel was produced by the asymmetric chemical ion-track-etching of a 12 μm thick polyethylene terephthalate (PET) membrane containing a single ion track in the center. The resulting conical nanochannel had a large base diameter of ~1000 nm and a narrow tip diameter of ~40–60 nm (Fig. S1, ESI†).

[a] *Department of Chemical and Biomolecular Engineering, The University of Akron, Akron, Ohio 44325, USA. E-mail: zhengj@uakron.edu*
[b] *College of Polymer Science and Polymer Engineering, The University of Akron, Akron, Ohio 44325, USA*
[c] *R&D Center for Membrane Technology and Department of Chemical Engineering, Chung Yuan Christian University, Chung-Li, Taoyuan 320, Taiwan*

† Electronic supplementary information (ESI) available: Experimental sections and additional figures. See DOI: 10.1039/c3cc44249g

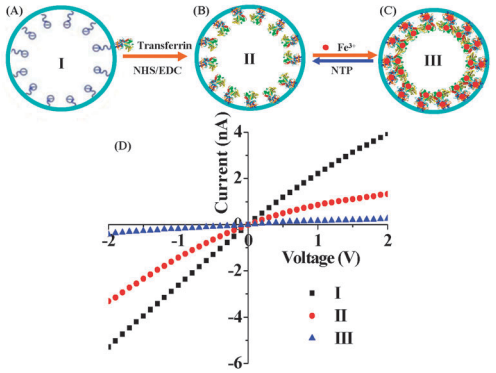


**Fig. 1** Schematic representation of a biomimetic iron-responsive nanochannel in a PET film using a chemical modification route to produce the interior surface modified by different molecules. (A) Single conical-shaped Nanochannel-I coated with COOH groups using a track-etching technique. (B) Nanochannel-II by the covalent attachment of the apo-Tf on carboxyl groups *via* carbodiimide coupling chemistry. (C) Nanochannel-III with iron binding to the apo-Tf. (D) Current–voltage (*I–V*) properties of the single Nanochannel-I, II, and III using PBS as electrolyte.

Fig. 1A and B showed that during the chemical etching process, carboxyl groups were first generated on the nanochannel surface (defined as Nanochannel-I), followed by covalent immobilization of apo-Tf molecules onto the inner surface of the same channel by a classical EDC/NHS coupling reaction (Nanochannel-II). Nanochannel-II was then incubated in a $FeCl_3$ aqueous solution (0.75 mM, pH = 4.3) for 1 hour to generate a holo-Tf (*i.e.* $Fe^{3+}$–apo-Tf-complex) functionalized Nanochannel-III (Fig. 1C). Fig. 1D shows remarkable differences in current–voltage (*I–V*) curves for Nanochannel-I-II-III at three different states under the same experimental condition of 10 mM PBS (pH 7.4) as the electrolyte. All three nanochannels exhibited almost linear symmetry *I–V* characteristics, and the ionic current flowing through the nanochannels was significantly decreased from Nanochannel I to III, confirming the success of the stepwise surface modifications of the bare PET nanochannel. From Nanochannel I to II, the change of ionic current was caused by the conjugation of apo-Tf onto the interior surface of the COOH-coated nanochannel resulting in the decrease in effective pore size, and therefore the ionic current was reduced correspondingly. From Nanochannel II to III, the binding of $Fe^{3+}$ onto the apo-Tf would induce the structural transition of apo-Tf to a more compact structure[18] on the inner surfaces of the nanochannel, which can decrease the effective pore size, resulting in low conductivity. Additionally, the formation of $Fe^{3+}$–apo-Tf complexes on the nanochannel also changed the surface charge and the surface charge distribution of the nanochannel, which in turn control channel conductivity. Parallel experiments were conducted to confirm that $Fe^{3+}$ ions do not bind to the COOH-coated Nanochannel-I even after $Fe^{3+}$ treatment (Fig. S2, ESI†). Further, to test the ion selectivity of the nanochannel, we incubated the apo-Tf functionalized Nanochannel-II in a NaCl solution (0.75 mM) and a PBS buffer containing NaCl and KCl (pH 7.4, 10 mM) for 1 hour, respectively, no significant change in the ionic current was observed (Fig. S3, ESI†), indicating that the apo-Tf functionalized nanochannel indeed exhibits a selective binding to $Fe^{3+}$ ions. Other stimuli-responsive nanochannels also displayed similar *I–V* behaviors.[19,20]

Considering the difficulties in characterizing the physicochemical properties of the surface coating inside the nanochannel, we conducted parallel characterizations on the surface properties of the COOH-SAM-coated gold surface and sodium hydroxide etched PET film before and after surface modifications by apo-Tf, corresponding to the respective surface coatings of Nanochannel I and II. First, we used a surface plasmon resonance (SPR) sensor to real-time monitor the covalent attachment of apo-Tf molecules onto a COOH-SAM-coated gold surface. As shown in Fig. S4A (ESI†), carboxyl groups of COOH-SAM coated on SPR chips were first activated by the injection of a freshly prepared aqueous solution of 15 mg EDC and 3 mg NHS per milliliter for 30 min at room temperature. DI water was injected to obtain a stable baseline. A 2 mg $mL^{-1}$ apo-Tf solution was flowed over spots of the activated COOH-SAM for 1 hour, followed by washing with DI water to remove unbound or loosely bound proteins. A typical SPR sensorgram showed a ~20 nm wavelength shift before and after the apo-Tf injection, corresponding to ~340 ng $cm^{-2}$ apo-Tf covalently attached onto the COOH-SAM-coated gold substrate.

Surface wettability of the PET films sequentially modified by NaOH (9 mM) solution, NHS–EDC solution and apo-Tf (2 mg $mL^{-1}$) solution (corresponding to the same surface modification of Nanochannels I and II) was further examined by water contact angle measurements. Visual inspection of the surface wettability clearly showed a visible change of contact angles on four different PET films. The mean water contact angle was 77.3 ± 4.3° on the untreated PET film (Fig. S4-B2, ESI†). Upon incubation of the untreated PET film in a NaOH solution (9 M) for 4 hours, the contact angle decreased to 32.1 ± 2.2° (Fig. S4-B3, ESI†), indicating the formation of a much more hydrophilic COOH-covered surface on the PET film. The NaOH-etched PET film was further treated with a solution of 15 mg EDC and 3 mg NHS per milliliter for 1 hour at room temperature to initiate the EDC–NHS reaction, and the resulting contact angle of NHS–EDC-activated PET film was changed to 43.4 ± 1.2° (Fig. S4-B4, ESI†), indicating the conversion of –COOH groups to NHS ester groups. Finally, when treating the NHS–EDC-activated PET film with an apo-Tf aqueous solution of 2 mg $mL^{-1}$ overnight, the contact angle of apo-Tf-modified PET film decreased to 23.2 ± 1.5° (Fig. S4-B5, ESI†), indicating the successful conjugation of apo-Tf onto the PET film. Thus, the changes of water contact angles also reflect the changes of the surface chemical compositions of the modified PET films.

The specific $Fe^{3+}$ responsive property of the apo-Tf functionalized nanochannel was investigated using fluorescence spectroscopy. Upon selective binding of irons to apo-Tf, apo-Tf undergoes a conformational change with Trp residues exposed to the environment, which will decrease the fluorescence intensity of apo-Tf, leading to a direct correlation between iron-binding-induced conformational changes and fluorescence intensity. Fig. 2 compares the fluorescence intensity

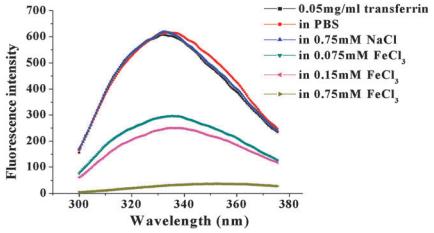


**Fig. 2** Fluorescence intensity of a fixed concentration of apo-Tf (0.05 mg $mL^{-1}$) in different ionic solutions.

 

of a fixed concentration of apo-Tf (0.05 mg $mL^{-1}$) in different ionic solutions. When the apo-Tf was dissolved in DI water, NaCl solution (0.75 mM), and PBS buffer containing NaCl and KCl, separately, the fluorescence curves were almost identical and no fluorescence change was observed. The fluorescence independence of solvent conditions suggests that $Na^+$ and $K^+$ ions do not involve binding interactions with apo-Tf and induce the conformation change of apo-Tf, so that Trp residues are well shielded from other residues. Conversely, when dissolving apo-Tf in $FeCl_3$ solutions of different concentrations, fluorescence intensities were progressively decreased as the $FeCl_3$ concentrations increased from 0.075 to 0.75 mM. The most significant decrease in fluorescence occurred in 0.75 mM $FeCl_3$ solution, instead of in 0.075 and 0.15 mM $FeCl_3$ solutions, suggesting more numerous and stronger bindings formed between $Fe^{3+}$ ions and the unfolded apo-Tf, due in part to greater Coulombic repulsion in the higher $Fe^{3+}$ ionic concentrations. More importantly, compared to the unchanged fluorescence in non-$Fe^{3+}$ solutions, the fluorescence decrease in $FeCl_3$ solutions further confirms that apo-Tf indeed selectively binds to $Fe^{3+}$, not $Na^+$ and $K^+$, as evidenced by the decreased fluorescence density.

In living systems, the reversible binding and unbinding of $Fe^{3+}$ to Tf can (re)cycle over 100 times for iron delivery. Although the exact mechanism for such an overwhelming iron binding–unbinding process still remains unclear, it was proposed[21] that the $Fe^{3+}$–apo-Tf complex can go through a conformational change from a closed to an open state, and the open state is presumed to be the only conformation capable of forming the mixed ligand intermediate, which can further dissociate into the $Fe^{3+}$–ligand complex and apo-Tf, resulting in the removal of $Fe^{3+}$ from Tf. To mimic the reversible binding–unbinding process between $Fe^{3+}$ and Tf using the nanochannel, nitrilotri(methylphosphonic acid) (NTP) (Scheme S1, ESI†) was used as a ligand to remove $Fe^{3+}$ from Tf *via* a ligand exchange reaction, presumably due to a high binding affinity of NTP with $Fe^{3+}$. Fig. 3A shows the open–closed switching ability of the nanochannel for ionic conductivity upon alternately binding and unbinding of $Fe^{3+}$ to and from Tf. After treating the Nanochannel II (*i.e.* apo-Tf functionalized nanochannel) with a $FeCl_3$ solution (0.75 mM) for 1 hour, $Fe^{3+}$ will specifically bind to Tf causing a decrease of ionic current flowing through the nanochannel from 1.3 nA to 0.3 nA at 2 V using PBS as an electrolyte. Upon $Fe^{3+}$ binding to apo-Tf, which changes the Nanochannel-II to the Nanochannel-III, the Nanochannel-III was then treated with an NTP solution (200 mM) for 1 hour to remove $Fe^{3+}$ from Tf, resulting in the ionic current changing back to 1.3 nA. This reversible and switchable $Fe^{3+}$ binding–unbinding process in the nanochannel can be reproduced repeatedly for 5 cycles, reflecting a protein-conformation-gating ionic transport property.

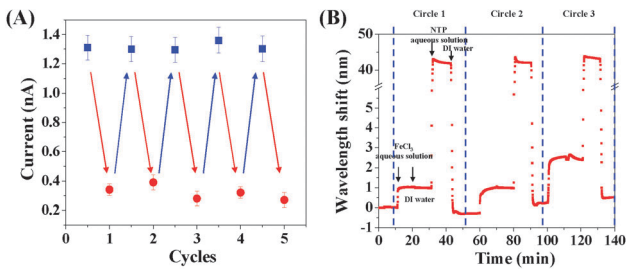


**Fig. 3** (A) Five reversible cycles of the ionic current transport through a single apo-Tf functionalized nanochannel at 2 V. (B) Three SPR detecting cycles of binding and unbinding of $Fe^{3+}$ to the apo-Tf functionalized COOH-SAM-coated gold substrate. Each circle consists of $Fe^{3+}$ binding by $FeCl_3$ injection, DI water washout, $Fe^{3+}$ removal by NTP injection, and additional DI water washout for surface regeneration.

This reversible binding and removal of $Fe^{3+}$ from the Tf was further tested on the apo-Tf functionalized gold chip. Fig. 3B shows three SPR detecting cycles, and each cycle comprises $Fe^{3+}$ binding by $FeCl_3$ injection, DI water washout, $Fe^{3+}$ removal by NTP injection, DI water washout, and surface regeneration. Each SPR cycle always began with an injection of DI water flowing through the apo-Tf-coated chip to establish the stable baseline. In cycle 1, injection of a $FeCl_3$ solution (0.75 mM), followed by DI water washing, led to an SPR wavelength shift of ~1 nm, indicating the binding of $Fe^{3+}$ to the apo-Tf. Then, upon injection of an NTP solution (200 mM), a large wavelength shift of 40 nm was observed, indicating that NTP ligands are immobilized onto the apo-Tf. The subsequent DI water wash caused the baseline to return to its original value, indicating that the attached $Fe^{3+}$ ions were completely removed. At this point, the SPR chip is ready to use in the next cycle. In cycles 2 and 3, similar behaviors of $Fe^{3+}$ binding and unbinding were observed, consistent with multiple reversible iron-binding–unbinding cycles in the nanochannel.

In summary, we developed a new iron-responsive nanochannel to mimic a multiple and reversible binding and unbinding process between Fe ions and transferrins. Integration of apo-Tf into the nanochannel demonstrates a protein-conformation-gating mechanism, which governs the selective binding–unbinding of $Fe^{3+}$ in a reproducible and reversible manner.

This work was supported by NSF-CAREER Award CBET-0952624 and NSF-CBET-1158447.

## Notes and references

1 T. M. Fyles, *Chem. Soc. Rev.*, 2007, **36**, 335–347.
2 Z. S. Siwy, M. R. Powell, E. Kalman, R. D. Astumian and R. S. Eisenberg, *Nano Lett.*, 2006, **6**, 473–477.
3 X. Hou, W. Guo and L. Jiang, *Chem. Soc. Rev.*, 2011, **40**, 2385–2401.
4 X. Hou, H. Dong, D. Zhu and L. Jiang, *Small*, 2010, **6**, 361–365.
5 X. Hou, W. Guo, F. Xia, F.-Q. Nie, H. Dong, Y. Tian, L. Wen, L. Wang, L. Cao, Y. Yang, J. Xue, Y. Song, Y. Wang, D. Liu and L. Jiang, *J. Am. Chem. Soc.*, 2009, **131**, 7800–7805.
6 C. Han, X. Hou, H. Zhang, W. Guo, H. Li and L. Jiang, *J. Am. Chem. Soc.*, 2011, **133**, 7644–7647.
7 E. B. Kalman, I. Vlassiouk and Z. S. Siwy, *Adv. Mater.*, 2008, **20**, 293–297.
8 D. Wendell, P. Jing, J. Geng, V. Subramaniam, T. J. Lee, C. Montemagno and P. Guo, *Nat. Nanotechnol.*, 2009, **4**, 765–772.
9 B. Zhang, Y. H. Zhang and H. S. White, *Anal. Chem.*, 2004, **76**, 6229–6238.
10 J. H. Yuan, F. Y. He, D. C. Sun and X. H. Xia, *Chem. Mater.*, 2004, **16**, 1841–1844.
11 A. J. Storm, J. H. Chen, X. S. Ling, H. W. Zandbergen and C. Dekker, *Nat. Mater.*, 2003, **2**, 537–540.
12 P. Apel, *Radiat. Meas.*, 2001, **34**, 559–566.
13 Y. Tian, Z. Zhang, L. Wen, J. Ma, Y. Zhang, W. Liu, J. Zhai and L. Jiang, *Chem. Commun.*, 2013, DOI: 10.1039/C3CC42748J.
14 Y. Tian, X. Hou, L. Wen, W. Guo, Y. Song, H. Sun, Y. Wang, L. Jiang and D. Zhu, *Chem. Commun.*, 2010, **46**, 1682–1684.
15 Z. Siwy, L. Trofin, P. Kohli, L. A. Baker, C. Trautmann and C. R. Martin, *J. Am. Chem. Soc.*, 2005, **127**, 5000–5001.
16 R. Engle-Stone, M. Nankap, A. O. Ndjebayi, J. G. Erhardt and K. H. Brown, *J. Nutr.*, 2013, **143**, 369–377.
17 A. Yersin, T. Osada and A. Ikai, *Biophys. J.*, 2008, **94**, 230–240.
18 F. Kilar and I. Simon, *Biophys. J.*, 1985, **48**, 799–802.
19 M. Ali, P. Ramirez, S. Mafé, R. Neumann and W. Ensinger, *ACS Nano*, 2009, **3**, 603–608.
20 M. Ali, B. Yameen, R. Neumann, W. Ensinger, W. Knoll and O. Azzaroni, *J. Am. Chem. Soc.*, 2008, **130**, 16351–16357.
21 W. R. Harris, *J. Inorg. Biochem.*, 1984, **21**, 263–276.